ELSEVIER

Computers and Geotechnics 30 (2003) 489–503

COMPUTERS AND GEOTECHNICS

www.elsevier.com/locate/compgeo

# An approach to estimate unsaturated shear strength using artificial neural network and hyperbolic formulation

S.J. Lee[a], S.R. Lee[a,*], Y.S. Kim[b]

[a]*Department of Civil and Environmental Engineering, Korea Advanced Institute of Science and Technology (KAIST), 373-1 Kusong-dong, Yusong-gu, Daejeon, 305-701, South Korea*

[b]*Division of Ocean System, Yosu National University, San 96-1, Dundeok-dong, Yeosu, Jeonnam, 550-749, South Korea*

Received 5 June 2002; received in revised form 7 February 2003; accepted 25 March 2003

**Abstract**

Since most soils exist above the ground water table, negative pore water pressures develop in unsaturated soils. This negative pore water pressure, known as matric suction, causes increased shear strength. Therefore, it is required that the effect of the increase in shear strength should be included in geotechnical analyses. However, experimental studies on unsaturated soils are generally costly, time-consuming, and difficult to conduct. Therefore, it is better to have an empirical method that is able to predict the unsaturated shear strength with respect to the matric suction in a more convenient way. For that purpose, we formulated a nonlinear unsaturated shear strength relationship with the matric suction in a hyperbolic form. In the formulation, conventional saturated soil parameters ($c'$, $\phi'$) and an ultimate increment of apparent cohesion ($C_{max}$) are required. A method is also developed wherein $C_{max}$ can be predicted using an ANN (artificial neural network) in reference to data obtained from tests conducted in this study and published in references.

© 2003 Elsevier Science Ltd. All rights reserved.

*Keywords:* Apparent cohesion; Unsaturated shear strength; Hyperbolic formulation; Artificial neural network

## 1. Introduction

Generally the saturated shear strength of soils, expressed by the Mohr–Coulomb criterion, has been applied to predictions of slope stability, bearing capacity, and earth pressure, and in the analysis of field test data such as PMT, SPT, etc. However, concerns with the contribution of matric suction to the shear strength of unsaturated soils have been growing during recent decades, and hence a considerable number of studies have been conducted on unsaturated soils. Accordingly unsaturated soil behavior could be more reasonably predicted by considering the matric suction.

However, Vanapalli et al. [44] mentioned that although shear strength theories for unsaturated soils have been formulated and they seem to be consistent with observed experimental behavior, the experimental measurements of shear strength for an unsaturated soil are time-consuming and require costly laboratory facilities. This has limited, to a certain degree, the application of shear strength theories developed for unsaturated soils into research and academic areas. Thus there have been limited practical applications of the unsaturated shear strength theory. It is therefore important to develop a simpler approach for predicting the shear strength of an unsaturated soil for various engineering applications.

Some attempts have also been made to predict the shear strength of an unsaturated soil using empirical procedures. Abramento and Carvalho [1] used a curve fitting technique for representing their experimental data. They used an exponential function that retains the form of the shear strength equation proposed by Fredlund et al. [12], treating $\tan\phi^b$ as a variable with respect to the matric suction. Vanapalli et al. [44] developed an empirical and analytical model to predict nonlinear shear strength in terms of soil suction. The formulation makes use of a soil water characteristic curve, saturated shear strength parameters, and an empirical parameter, $\kappa$. Öberg and Sällfors [32] roughly replaced the $\chi$-parameter

* Corresponding author. Tel.: +82-42-869-3617; fax: +82-42-869-3610.

*E-mail address:* srlee@kaist.ac.kr (S.R. Lee).

0266-352X/03/$ - see front matter © 2003 Elsevier Science Ltd. All rights reserved.
doi:10.1016/S0266-352X(03)00058-2

that Bishop [2,3] introduced, by $S_r$ (degree of saturation). Khalili [22] introduced a unique relationship between the effective stress parameter, $\chi$ and the ratio of suction over the air entry value, and proposed a method to estimate the unsaturated shear strength using this parameter with cohesion, friction angle and confining pressure. Rassam and Williams [38] proposed a function that describes the shear strength of unsaturated soils in terms of matric suction and normal stress, based on three-dimensional nonlinear regression analysis results. It incorporates the effect of normal stress on the contribution of matric suction to shear strength.

The existing methods need additional tests for unsaturated soils such as unsaturated shear strength tests or SWCC[1] tests, in order to predict the nonlinear characteristics of the shear strength of the unsaturated soil. However, since these tests for unsaturated soils are very difficult, time-consuming and costly to conduct, it is practically difficult to apply for predicting the shear strength by them, even though the shear strength of the unsaturated soils could be represented by the most of these methods. Therefore, we intended to propose a simple function to represent the shear strength characteristics of unsaturated soil, and to propose a method to predict the unsaturated shear strength on the basis of the simple function, without conducting additional tests for unsaturated soils.

To sum up, the objectives of this paper are (1) to propose a simple equation for representing unsaturated shear strength with an additional parameter possessing physical meaning, and (2) to propose a new method to predict the only one parameter required to represent the shear strength of an unsaturated soil without any additional tests for unsaturated soils.

For that purpose we proposed a simple shear strength equation in a hyperbolic form for unsaturated soils using an extended Mohr–Coulomb equation, based on the previously published research results. The increased shear strength of unsaturated soils, referred to apparent cohesion, nonlinearly increasing with the matric suction, can be represented by only one parameter, $C_{max}$ in this equation. The proposed equation was verified by saturated and unsaturated triaxial test results for weathered granite soils, commonly found in Korea. Based on the formulation, we proposed a method to estimate the ultimate increment of apparent cohesion ($C_{max}$) for the unsaturated soils from several basic soil properties, using an ANN (artificial neural network) without carrying out any additional unsaturated shear strength tests.

[1] 'SWCC' is an abbreviation for 'Soil Water Characteristic Curve.' SWCC is commonly defined as the relationship between the water content and the matric suction of a soil, and used in order to predict the parameters of unsaturated soils such as the unsaturated coefficient of permeability and the unsaturated shear strength.

## 2. Shear strength of unsaturated soils

Fredlund et al. [12] introduced an unsaturated shear strength criterion using two different friction angles, where an additional friction angle $\phi^b$ is assumed to be related to the matric suction as

$$\tau_f = c' + (\sigma - u_a)\tan\phi' + (u_a - u_w)\tan\phi^b \quad (1)$$

in which $\tau_f$ is shear stress at failure, $c'$ is effective cohesion, $\phi'$ is friction angle, $\sigma$ is total stress, $u_a$ is pore-air pressure, $u_w$ is pore-water pressure, $(\sigma - u_a)$ is net normal stress, and $(u_a - u_w)$ is matric suction. However, the experimental results show nonlinear shear strength behavior when tests are performed over a wide range of suctions [10,14].

### 2.1. Hyperbolic formulation of apparent cohesion

During the shear tests under a set of constant matric suction and net normal stress, the soil specimen is compressed to a failure state. We can then construct a Mohr circle for the failure condition at each matric suction stage. A line tangent to the Mohr circles at failure conditions represents a failure envelope corresponding to the matric suction variation. The friction angle ($\phi'$) is assumed to be equal to the effective friction angle obtained from shear strength tests on saturated soils, for all the values of matric suctions [13,21,39]. The cohesion intercept at which the failure envelope intersects the shear strength versus matric suction plane, that is the $(\sigma - u_a) = 0$ plane, at a certain matric suction value, can be defined as an apparent cohesion corresponding to the matric suction (Fig. 1).

It has been found from earlier studies that $\phi^b$ appears to be equal to $\phi'$ at low matric suction, but decreases to a lower value at high matric suction. In other words, the apparent cohesion shows nonlinearity as a function of matric suction. We formulated the apparent cohesion variation as a hyperbolic type in order to consider the nonlinearity of apparent cohesion.

Figs, 1(b) and 2 show a hyperbolic curve defined by friction angle ($\phi'$), cohesion ($c'$) and the ultimate increment of apparent cohesion ($C_{max}$) in the matric suction versus shear strength plane. $C_{A,max}$ is an asymptote value of the hyperbolic equation and $C_{max}$ indicates an increase of apparent cohesion induced by matric suction. The hyperbolic equation can be formulated by initial slope ($1/a$) and the ultimate value ($1/b$) related to the friction angle ($\phi'$) and the ultimate increment of apparent cohesion ($C_{max}$), respectively. Since just one additional parameter is used for considering the unsaturated shear strength in this hyperbolic equation, the number of parameters to estimate is reduced to the minimum.

$$C_A = c' + \frac{(u_a - u_w)}{a + b(u_a - u_w)} \quad (2)$$

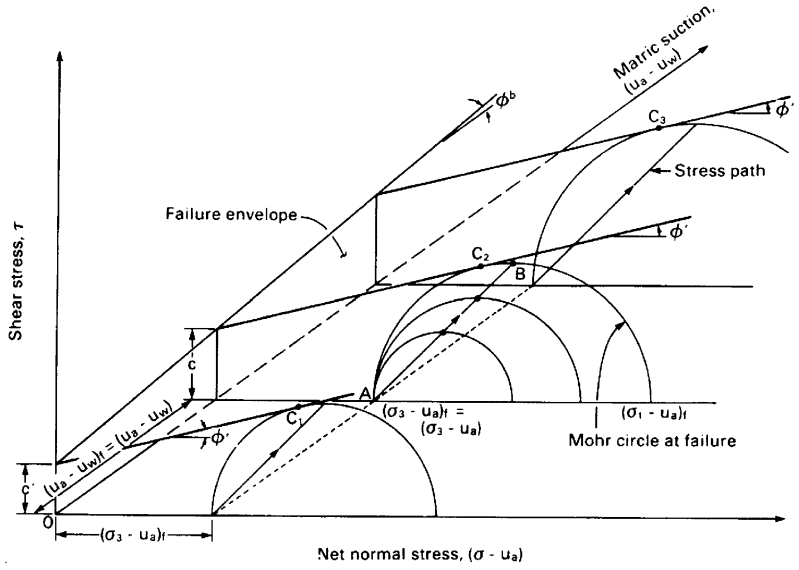


(a) Linear apparent cohesion by $\phi^b$ [13]

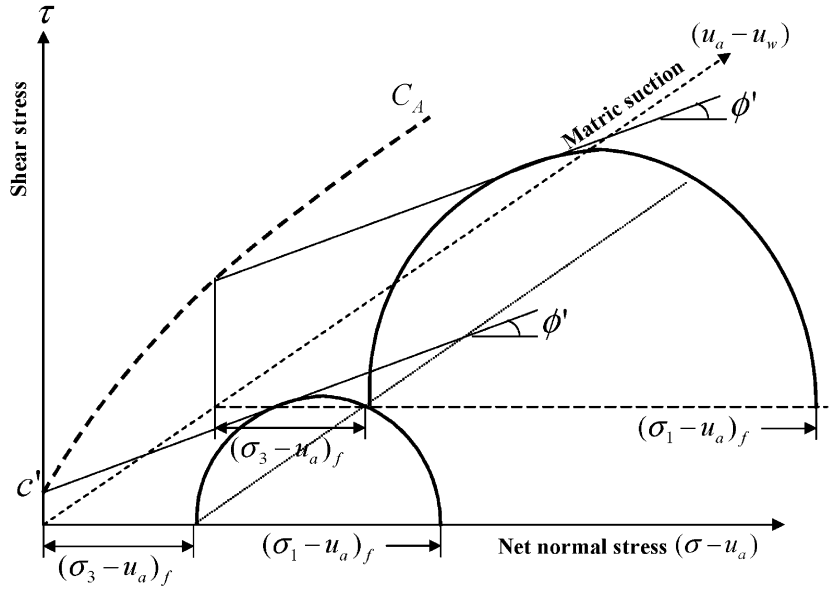


(b) Non-linear apparent cohesion by $C_{\max}$

Fig. 1. Stress paths followed during consolidated drained tests at various matric suctions under a constant net confining pressure [13].

$$C_{A,\max} = C_{\max} + c' \tag{3}$$

$$a = \frac{1}{\tan\phi'}, \quad b = \frac{1}{C_{\max}} \tag{4}$$

The equation was applied to test results obtained by several researchers (Table 1). Fig. 3 shows the hyperbolic equation with a suitable ultimate increment of apparent cohesion ($C_{\max}$) and the test results. We could recognize from the figure that the proposed hyperbolic equation well represents the apparent cohesion variation

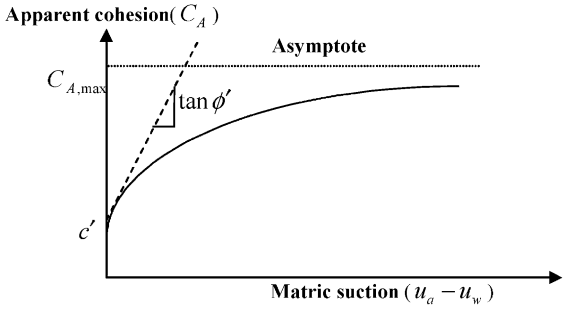


Fig. 2. Apparent cohesion represented by a hyperbolic curve.

of unsaturated soils with matric suction. Therefore, it can be expected that the nonlinear relationship between the apparent cohesion and matric suction may simply, yet effectively predict the unsaturated shear strength.

### 2.2. Triaxial tests for unsaturated soils

Consolidated drained triaxial tests for unsaturated soils were conducted by modifying an existing triaxial test apparatus for saturated soils. The negative pore water pressure is maintained in order to induce the matric suction, using the axis-translation technique [18]. In a triaxial cell, the pore air pressure ($u_a$) is usually controlled through a porous stone placed at top of the soil specimen. The pore water pressure ($u_w$) is controlled through a saturated high air entry ceramic disk sealed to the pedestal of the triaxial cell. In this way, the matric suction ($u_a-u_w$) retains a constant value. The air entry value of the ceramic disk used in this test is 5 bar (≈500 kPa).

The specimens for saturated and unsaturated triaxial tests were prepared by a kneading compaction technique. We used weathered granite soil samples collected from Okchun, Chochiwon, Yungi, and Seochang areas in Korea. Internal friction angles ($\phi'$) appear to be practically the same for various matric suctions, although the angle value slightly increases as the matric suction increases [13,21,39]. Therefore, we can conjecture that the matric suction has a small effect on the friction angle but a large effect on the apparent cohesion.

The consolidated drained triaxial tests should be carried out at low strain rate, in order to completely dissipate pore water pressures developed in the specimen during the shearing stage [8]. We selected 0.004 (mm/min) as an appropriate strain rate for the weathered granite soils, as proposed by Ho and Fredlund [19]. A multistage triaxial test technique was also used for the specimens at a constant net confining pressure ($\sigma_3-u_a$) for various matric suctions ($u_a-u_w$) to minimize the effect of variability of the specimen on the test results [13,36].

Matric suctions were varied from 50 to 400 kPa considering the air entry value of the ceramic disk, while the net normal stress was maintained at 100 kPa [27,28]. The apparent cohesions obtained from the unsaturated triaxial tests were summarized in Table 2. Fig. 4 presents some test results compared with the hyperbolic representation. This figure also clearly shows that the proposed hyperbolic equation well reproduces the test results.

## 3. Prediction of unsaturated shear strength using an artificial neural network

From what we have discussed previously, we could ascertain that the shear strength of unsaturated soils can be represented by conventional shear strength parameters ($c'$and $\phi'$) of saturated soils and an appropriate empirical parameter ($C_{max}$) using the hyperbolic formulation. Consequently, if a reliable method to predict the ultimate apparent cohesion ($C_{max}$) could be developed, one would be able to easily estimate the unsaturated shear strength. This would encourage the use of unsaturated shear strength theories in geotechnical engineering practices.

Table 1
Soil properties and shear strength data obtained by several researchers

| Gravel (%) | Sand (%) | Silt + clay (%) | Void ratio | Compacted water content (%) | | $c'$ (kPa) | $\phi'$ (°) | OMC (%) | $C_{max}$ (kPa) | References |
|---|---|---|---|---|---|---|---|---|---|---|
| | | | | Real value | Input value[a] | | | | | |
| 0 | 28 | 72 | 0.77 | 11.83 | −4.17 | 10 | 25.5 | 16 | 150 | Gan et al. [15] |
| 0 | 28 | 72 | 0.53 | 11.5 | −4.5 | 10 | 25.5 | 16 | 300 | |
| 0 | 28 | 72 | 0.69 | 12.27 | −3.73 | 10 | 25.5 | 16 | 280 | |
| 0 | 28 | 72 | 0.51 | 12.23 | −3.77 | 10 | 25.5 | 16 | 300 | |
| 0 | 13.5 | 86.5 | 0.672[b] | 13.6 | −3.4 | 23.7 | 22.5 | 17 | 300 | Escario and Saez [9,10] |
| 0 | 5 | 95 | 0.666[b] | 21.5 | 0 | 0 | 35 | 21.5 | 200 | Krahn et al. [24] |
| 0 | 87.78 | 12.26 | 0.62 | 22.7 | 0 | 0 | 41.7 | – | 40 | Rassam and William [38] |
| 0 | 71.17 | 28.63 | 0.62 | 22.7 | 0 | 0 | 40.7 | – | 43 | |
| 0 | 28 | 72 | 0.517 | 16.3 | 0 | 0.56 | 22.19 | 16.3 | 200 | Vanapalli et al. [44] |
| 0 | 28 | 72 | 0.578 | 13 | −3.3 | 0 | 22.9 | 16.3 | 80 | |
| 0 | 28 | 72 | 0.542 | 19.2 | 2.9 | 0.22 | 23.18 | 16.3 | 230 | |
| 0 | 5 | 95 | 0.677 | 22.2 | 0 | 7.8 | 29 | – | 320 | Satija [40,41] |
| 2.6 | 50.3 | 47.1 | 1.15 | 24 | 0 | 0 | 26.4 | – | 120 | De-Campos and Carrillo [6] |
| 9.1 | 60 | 30.9 | 1.0 | 16.7 | 0 | 13.7 | 28.7 | – | 80 | |
| 0 | 4 | 96 | 0.63 | 18 | 0 | 25 | 22 | 18 | 270 | Cui and Delage [6] |
| 35 | 50.77 | 14.23 | 0.514 | 12 | 2 | 0.888 | 44.2 | 10 | 80 | Lee et al. [26] |

[a] The input values for the compacted water content were used by subtracting OMC from the real value. The input values were assumed for the soil that we did not have the OMC value.

[b] Void ratio($e$) estimated by an assumption of $G_s = 2.65$.

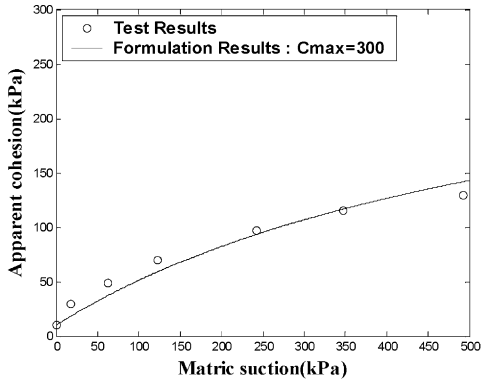


(a) Gan et al.[15] : GT-16-N4

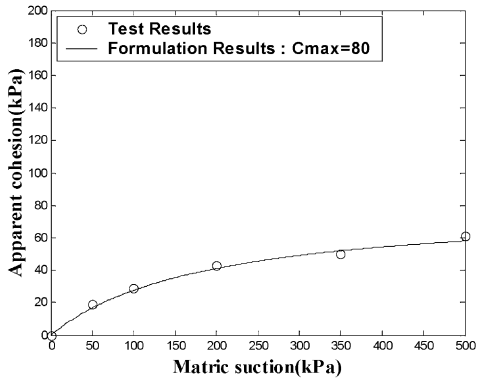


(b) Vanapalli et al.[44] : Galcial till(Dry)

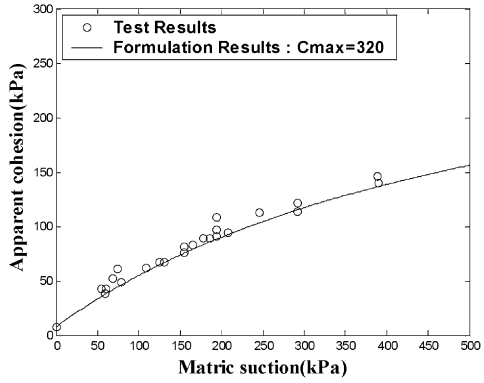


(c) Satija[40] : Dhanauri clay

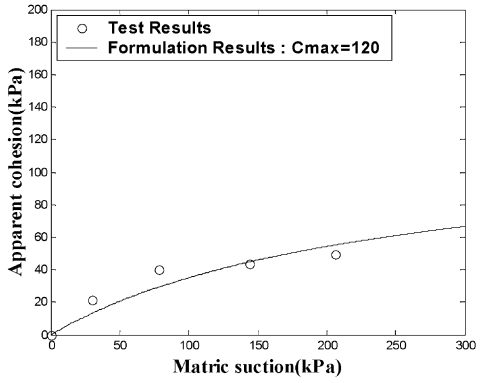


(d) De-Campos & Carrillo[6] : Colluvium

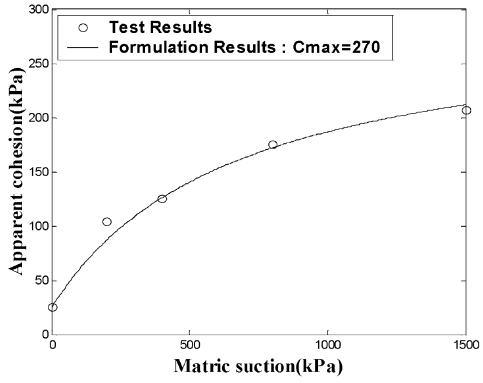


(e) Cui & Delage[5] : Jossigny silt

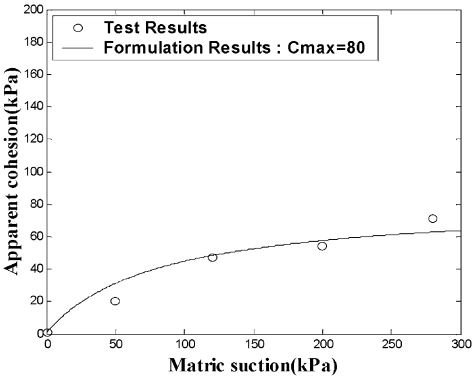


(f) Lee et al.[26]

Fig. 3. Hyperbolic representation for test results obtained by several researchers.

Hence, we proposed a method to estimate the ultimate increment of apparent cohesion ($C_{max}$) using an ANN (artificial neural network). We can recognize not only intuitively, but also from the test results that soil properties are interrelated, and have a complex influence on the increase in the unsaturated shear strength. To put it more concretely, we can generally see from the test results that the increment of apparent cohesion for identical soils is larger as the specimen is denser, finer, or compacted at wet side. Therefore, we used basic soil properties such as sand fraction, silt and clay fraction, void ratio, compaction condition, cohesion and friction angle, as input data in the ANN model for predicting the value of $C_{max}$.

### 3.1. Artificial neural network

#### 3.1.1. Overview of artificial neural network

Artificial neural networks are promising computational techniques capable of mapping and capturing all

Table 2
Soil properties and shear strength data obtained in this study

| Sites | Gravel (%) | Sand (%) | Silt + clay (%) | Void ratio | Compacted water content (%) | | $c'$ (kPa) | $\phi'$ (°) | OMC (%) | $C_{max}$ (kPa) |
|---|---|---|---|---|---|---|---|---|---|---|
| | | | | | Real value | Input value[a] | | | | |
| Okchun | 0.37 | 94.79 | 4.84 | 0.57 | 19.87 | 5.97 | 20.44 | 36.8 | 13.9 | 300 |
| | 0.37 | 94.79 | 4.84 | 0.57 | 7.93 | −5.97 | 22.51 | 34.6 | 13.9 | 75 |
| | 0.37 | 94.79 | 4.84 | 0.77 | 19.87 | 5.97 | 12.79 | 34 | 13.9 | 70 |
| Chochiwon | 0.98 | 92.59 | 6.43 | 0.673 | 23.78 | 7.53 | 20.49 | 34.35 | 16.25 | 230 |
| | 0.98 | 92.59 | 6.43 | 0.673 | 8.72 | −7.53 | 24.95 | 32.05 | 16.25 | 180 |
| | 0.98 | 92.59 | 6.43 | 1.0 | 23.78 | 7.53 | 18.2 | 31 | 16.25 | 210 |
| | 0 | 82.15 | 17.85 | 0.673 | 8.72 | −7.53 | 10.18 | 32.9 | 16.25 | 230 |
| Yungi | 5.74 | 92.71 | 1.56 | 0.48 | 18.77 | 5.14 | 17.15 | 41.21 | 13.63 | 95 |
| | 5.74 | 92.71 | 1.56 | 0.48 | 8.49 | −5.14 | 7.8 | 40.82 | 13.63 | 90 |
| | 0 | 95. 13 | 4.87 | 0.48 | 18.77 | 5.14 | 15.5 | 36.48 | 13.63 | 160 |
| Seochang | 0 | 78.71 | 13.89 | 0.606 | 20.61 | 8.11 | 5.97 | 36.04 | 12.5 | 95 |

[a] The input values for the compacted water content were used by subtracting OMC from the real value.

features and sub-features embedded in a large set of data that yields a certain output. A network that has successfully captured governing relationships between input and output data can be used as a prediction tool for cases where the output solution is not available. Therefore, training the network by presenting it with a set of examples constitutes an essential part of the network development phase. The input variables comprise the input layer to the network and the output layer contains the target output vector (the solution of the problem). A hidden layer, usually placed between the input and output layers, is usually employed to assist the network in the learning process. The nodes in a certain layer are connected to all nodes in the following and preceding layers [4,31].

A single-input neuron is shown in Fig. 5. The scalar input $p$ is multiplied by a scalar weight $w$ to form $wp$, one of the terms that is sent to the summer. The other input 1 is multiplied by a bias $b$ and then passed to the summer. The summer output $n$, often referred as the net input, goes into an activation function $f$, which produces the scalar neuron output $a$. The actual output depends on the particular activation function. Typically the activation function is chosen by the designer and then the parameters $w$ and $b$ are adjusted by a learning rule so that the neuron input/output relationship meets a specific goal.

### 3.1.2. Backpropagation algorithm [16]

The neural network adopted in this study uses the backpropagation algorithm. Backpropagation neural networks can provide accurate approximations to any continuous function with sufficient neurons [20]. Training is performed by repeatedly presenting the entire set of training patterns, updating the weights at the end of each training cycle until the average sum squared error over all the training patterns is minimized and within the tolerance specified for the problem. At the end of the training phase, the neural network should correctly reproduce the target output values for the training data, provided that the errors are minimal, i.e. that convergence occurs. The associated trained weights of the neurons are then stored in the neural network memory. In the next testing phase, the trained neural network is fed by a separate set of data. The neural network predictions using the trained weights are compared to the target output values to assess the ability of the neural network to produce correct responses for the testing patterns that only broadly resemble the data in the training set. Once the training and testing phases are found to be successful, the neural network can then be put to use in practical applications.

### 3.1.3. Generalization

One of the problems that occurs during the neural network training is called overfitting. The error on the training set is driven to a very small value, but when new data are presented to the network, the error can be large. However, if the number of parameters in the network is much smaller than the total number of points in the training set, then there is little or no chance of overfitting. Therefore, it is required to assemble as much data as possible. Otherwise, the reliability of neural network training can be guaranteed by using a generalization technique, when sufficient data cannot be collected [17]. Furthermore, generally some data collected is used for a training and other data may be used for validation. Thus, one may not sacrifice good data, but use all the data in the process of optimizing the parameters [29,30].

The generalization can be performed by the Bayesian regularization technique or early stopping. We used Bayesian regularization [29,30] in this study. The following

is the short description about the Bayesian regularization. Typically, training aims to reduce the sum of squared errors $F = E_D$. However, regularization adds an additional term; i.e. the objective function becomes $F = \beta E_D + \alpha E_W$, where $E_W$ is the sum of squares of the network weights, and $\alpha$ and $\beta$ are objective function parameters. The relative size of the objective function parameters dictates the emphasis for training. If $\alpha << \beta$, then the training algorithm will drive the errors smaller. If $\alpha >> \beta$, training will emphasize weight size reduction at the expense of network errors, thus producing a smoother network response [11].

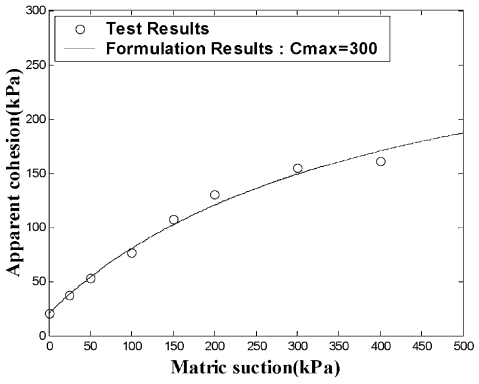


(a) Okchun soil(wet compaction, e=0.57)

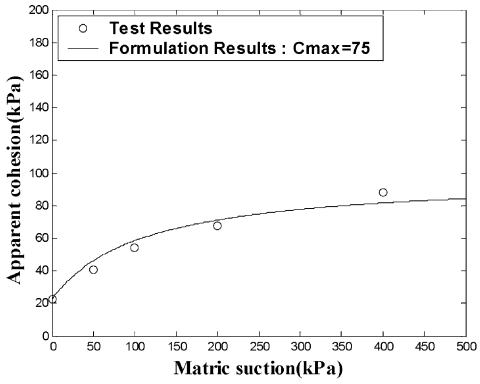


(b) Okchun soil(dry compaction, e=0.57)

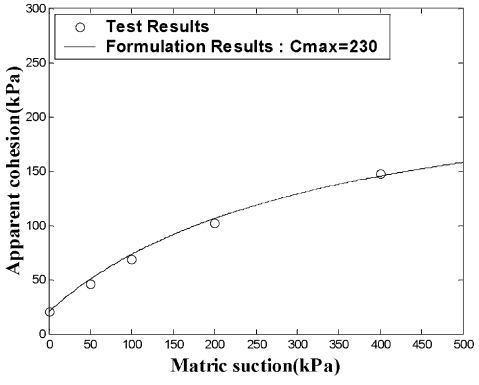


(c) Chochiwon soil(wet compaction, e=0.673)

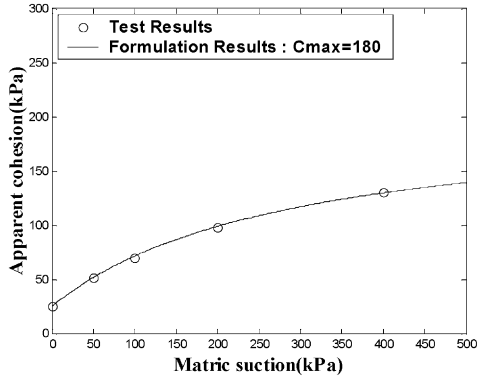


(d) Chochiwon soil(dry compaction, e=0.673)

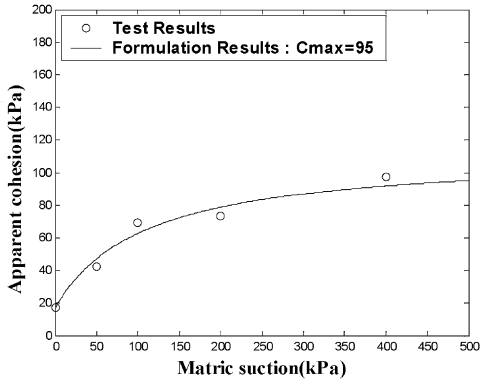


(e) Yungi soil(wet compaction, e=0.48)

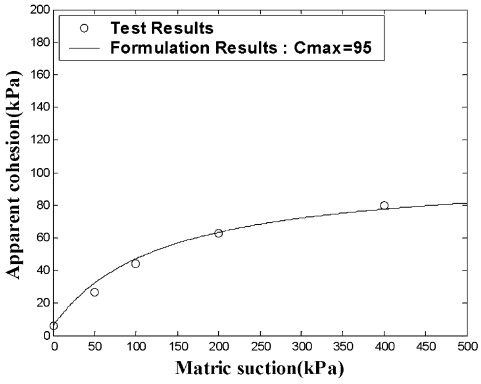


(f) Seochang soil(wet compaction, e=0.606)

Fig. 4. Test results and hyperbolic representation.

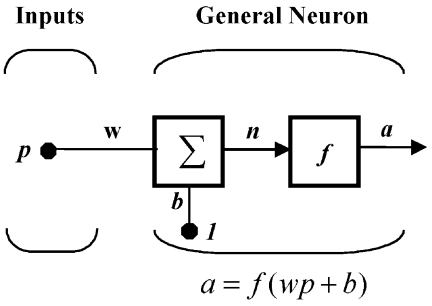


Fig. 5. Single-input neuron.

### 3.2. Application of ANN to the prediction of unsaturated shear strength

An ANN model learns from experimental data and forms neural connection strengths from a learning process, functioning somewhat like a human brain. Because of its unique learning, training and predicting characteristics, the ANN model has great potential applications in geotechnical engineering area particularly for situations where good experimental data are available. Thus several successful applications using ANN model have been reported [4,16,23,25,31,33,34,37,42,43].

#### 3.2.1. Database and architecture of ANN models

It was previously pointed out that basic properties of soils are interrelated, and affect the unsaturated shear strength (Tables 1 and 2). Therefore, we considered basic soil properties such as sand, silt and clay fractions based on USCS, void ratio, compacted water content, cohesion and friction angle as input parameters in the neural network model, and the tested ultimate increment of apparent cohesion ($C_{max}$) as a target. The toolbox of *Matlab* was used in the neural network process [7].

Sixteen unsaturated shear strength data sets (Table 1) collected from published studies and 11 data sets (Table 2) obtained through the tests in this study were evaluated by the neural network. Fig. 6 shows a typical 6–2–1 structure of the neural network used in this study.

With these 27 data sets and the earlier structure, we will discuss the results of neural network models trained under the following cases and propose the connection weights for each model.

1. 6–2–1 structure, 20 data sets (model I).
2. 5–2–1 structure(excluding the friction angle), 20 data sets (model II).
3. 5–2–1 structure(excluding the void ratio), 20 data sets (model III).
4. 5–2–1 structure(excluding the compacted water content), 20 data sets (Model IV).

The 6–2–1 structure has 6 nodes in the input layer, 2 nodes in the hidden layer, and 1 node in the output layer. The other 5–2–1 structure possesses 5 nodes in the input layer excluding an input parameter.

Before training, it is often useful to scale the inputs and targets so that they always fall within a specified range [35]. In this study, we scaled inputs and targets so that they fall in the range [−1, 1]. In other words, the minimum values of the original inputs and targets are scaled to '−1' and the maximum values of the original inputs and target are scaled to '1', respectively. After the network has been trained, the vectors that contain the minimum and maximum values of the original inputs and targets should be used to transform any future inputs that are applied to the network, just like the network weights and biases. Then the output of the network will be trained to produce outputs in the range [−1, 1], and we convert these outputs back into the same units that are used for the original targets. Whenever the trained network is used with new inputs they should be preprocessed with the minimum and maximum values computed for the training set. On the other hand, the activation function in the first layer is log–sigmoid activation function ($a = \frac{1}{1+e^{-n}}$), and the second (output) layer activation function is linear function ($a = n$), in this study.

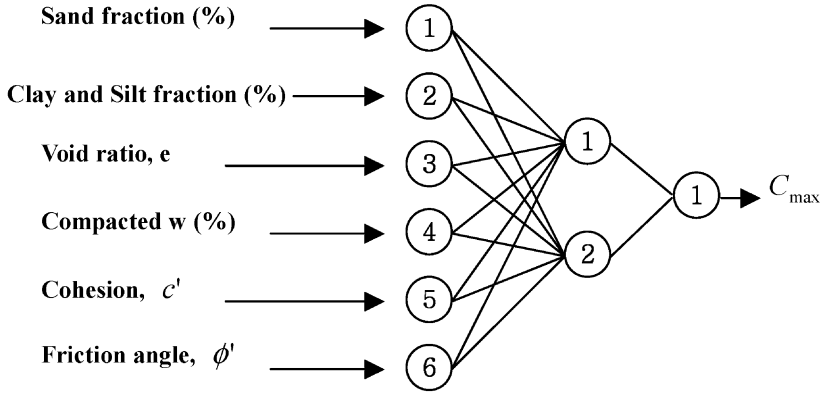


Fig. 6. An example of network structure (6–2–1) used in this study.

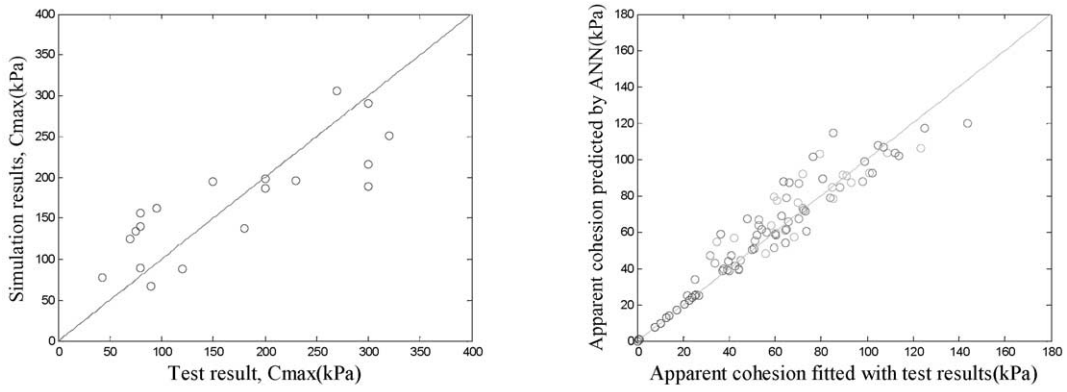


(a) Comparison of the $C_{max}$

(b) Apparent cohesions tested and estimated at various matric suctions

Fig. 7. ANN model I trained with 6–2–1 structure.

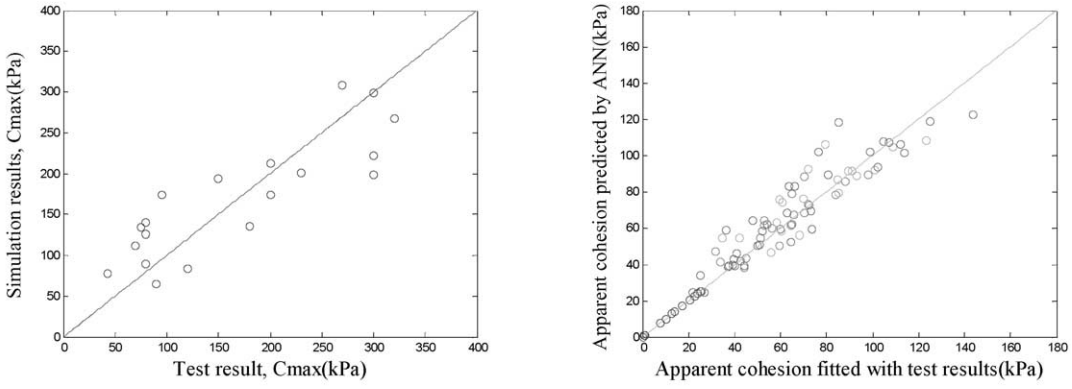


(a) Comparison of the $C_{max}$

(b) Apparent cohesions tested and estimated at various matric suctions

Fig. 8. ANN model II trained with 5–2–1 structure excluding the friction angle in the input layer.

### 3.2.2. Training of ANN models

An ANN model I was trained for 20 data sets using Bayesian regularization as a generalization technique with six input parameters in the input layer. Fig. 7(a) shows the results simulated by the neural network analysis and those obtained by the tests in regard to the ultimate increment of apparent cohesion ($C_{max}$). Fig. 7(b) shows a comparison of apparent cohesions obtained by the hyperbolic equation with the test results and the neural network simulation at various matric suction values.[2]

[2] In the beginning, we proposed a hyperbolic equation for representing the unsaturated shear strength, which uses one-parameter, $C_{max}$ to represent the apparent cohesion with the variation in matric suctions. In other words, we are able to compute apparent cohesion values in the whole range of matric suctions, if we can obtain a reliable $C_{max}$ for a specific soil. Thus, we intend to develop a method to predict $C_{max}$ and hence to compute apparent cohesions at each matric suction value using the $C_{max}$. The part (a) of the figure is the comparison between $C_{max}$ obtained by unsaturated shear tests and $C_{max}$ obtained by the simulation using the neural network. The part (b) of the figure is the comparison between apparent cohesion values by the test and apparent cohesion values by the simulation using the neural network at several matric suction values.

Preliminary parametric study showed that the effects of the friction angle ($\phi'$), the void ratio ($e$), and the compacted water content on the prediction of $C_{max}$ are relatively small in the neural network modeling, which will be discussed later. Accordingly, we trained 3 ANN models with 5–2–1 structure, excluding the friction angle, the void ratio ($e$), and the water content from the original input parameters in turn (model II–IV). Comparing Figs. 8, 9 and 10, there is little difference between the results of the 5–2–1 structure network model and those of the 6–2–1 structure network model. Table 4 shows a summary of comparison results obtained by the models that have different input variables and different structures.

### 3.2.3. Testing of ANN models

In order to see the applicability of the trained network models, they were tested to predict $C_{max}$ for data sets which were not introduced during the training stage [Figs. 11(a), 12(a), 13(a), 14(a) and Table 4]. Apparent cohesions were also computed with $C_{max}$ predicted from ANN and hyperbolic equation, and then compared with

the experimental test results [Fig. 11(b), 12(b), 13(b), and 14(b)]. As we can see in the results shown in the figures, the network model produces reliable predictions although the trained neural network models have used testing data sets that were not a part of the training data sets.

Based on these results, we could ascertain that it is reliable and appropriate to predict the apparent cohesion using the proposed hyperbolic equation and ANN models. Furthermore, we expect that the earlier ANN models will be reliable methods, even though we cannot

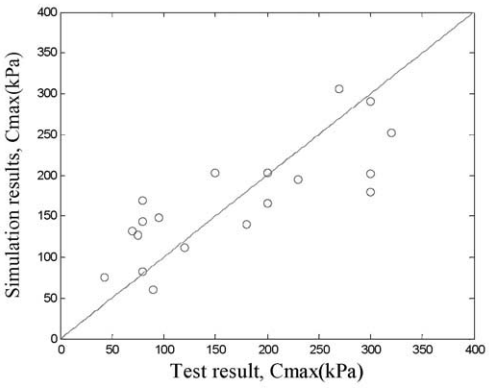


(a) Comparison of the $C_{max}$

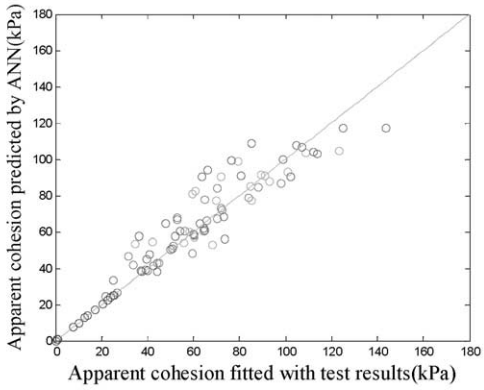


(b) Apparent cohesions tested and estimated at various matric suctions

Fig. 9. ANN model III trained with 5–2–1 structure excluding the void ratio in the input layer.

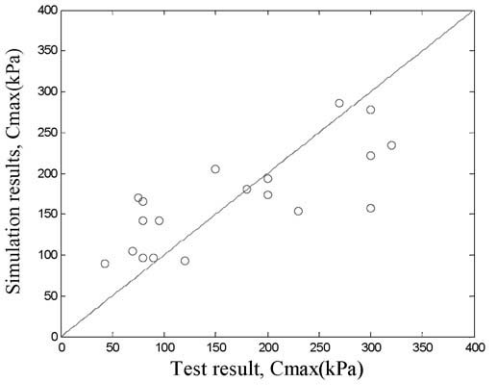


(a) Comparison of the $C_{max}$

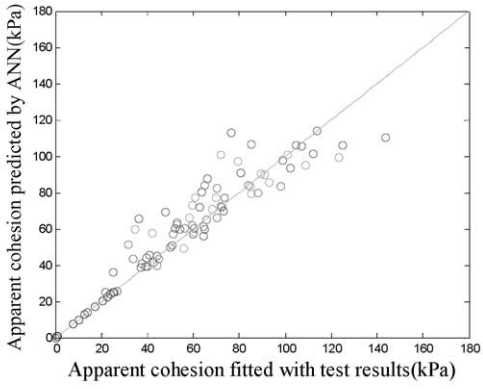


(b) Apparent cohesions tested and estimated at various matric suctions

Fig. 10. ANN model IV trained with 5–2–1 structure excluding the water content in the input layer.

Table 3
Summary of the results obtained by trained network models

| Model | Structure | Coefficient of determination ($R^2$) for $C_{max}$ | |
|---|---|---|---|
| | | $C_{max}$ by ANN model and test results | Apparent cohesion at various matric suctions by ANN model and test results |
| I | 6–2–1 | 0.67 | 0.91 |
| II | 5–2–1 (excluding friction angle) | 0.71 | 0.92 |
| III | 5–2–1 (excluding void ratio) | 0.64 | 0.91 |
| IV | 5–2–1 (excluding water content) | 0.58 | 0.89 |

Table 4
Summary of the results obtained by tested network models

| Model | Coefficient of determination ($R^2$) | |
|---|---|---|
| | $C_{max}$ by ANN model and test results | Apparent cohesion at various matric suctions by ANN model and test results |
| I | 0.90 | 0.93 |
| II | 0.88 | 0.93 |
| III | 0.95 | 0.91 |
| IV | 0.89 | 0.90 |

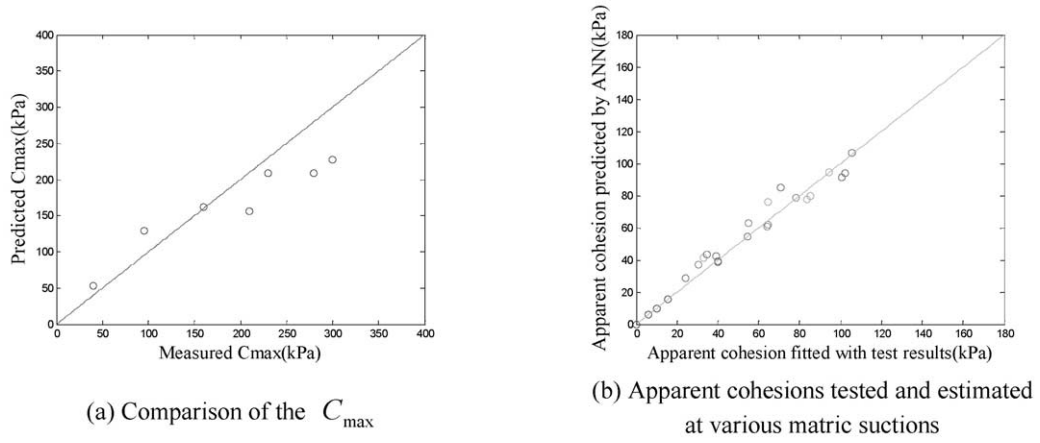


(a) Comparison of the $C_{max}$

(b) Apparent cohesions tested and estimated at various matric suctions

Fig. 11. Comparison of the results obtained by neural network model I and experimental tests.

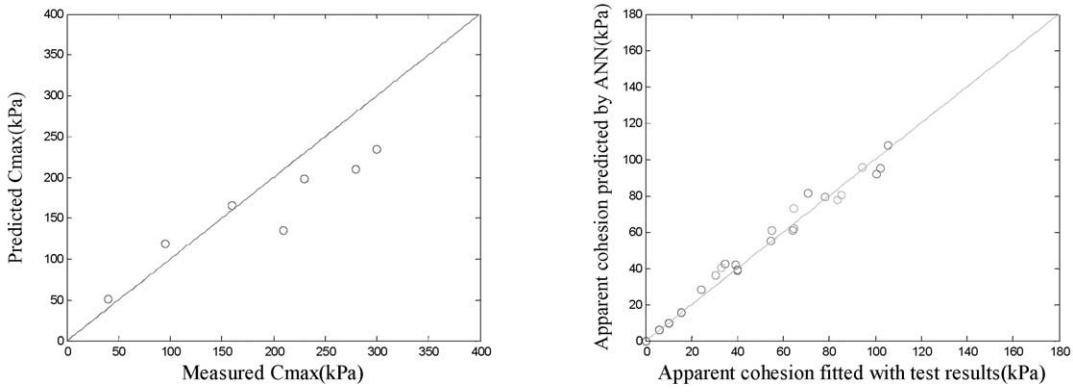


(a) Comparison of the $C_{max}$

(b) Apparent cohesions tested and estimated at various matric suctions

Fig. 12. Comparison of the results obtained by neural network model II and experimental tests.

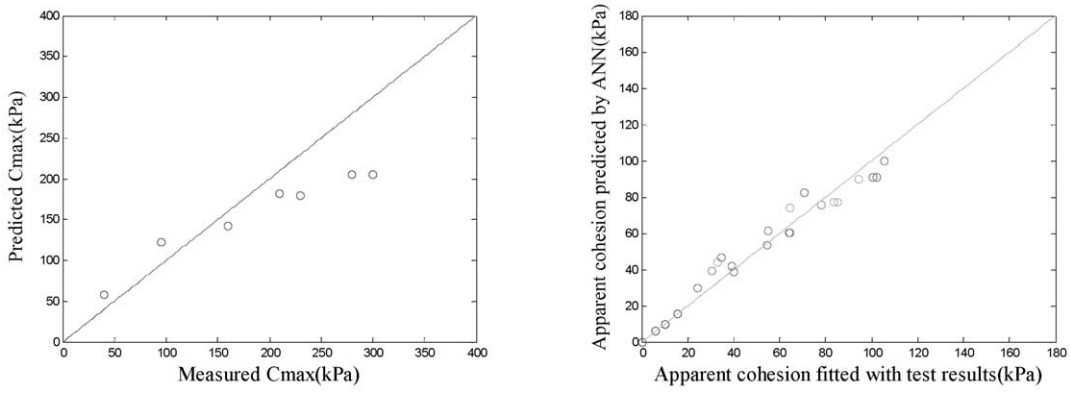


(a) Comparison of the $C_{max}$

(b) Apparent cohesions tested and estimated at various matric suctions

Fig. 13. Comparison of the results obtained by neural network model III and experimental tests.

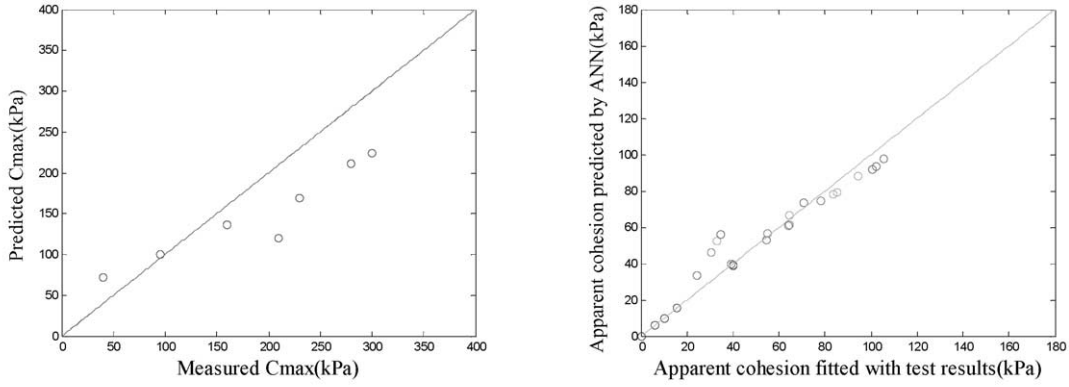


(a) Comparison of the $C_{max}$

(b) Apparent cohesions tested and estimated at various matric suctions

Fig. 14. Comparison of the results obtained by neural network model IV and experimental tests.

have data for one of three input parameters stated before. Besides, we exhibited the connection weights and biases for the neural network models trained in this study (Table 5). And, it is expected that the applicability for the prediction of unsaturated shear strengths would be more effective if we divide the soils into several groups and use the network model for each case.

### 3.2.4. Parametric study

Once an ANN model is evaluated, the ANN modeling provides a convenient way of conducting a parametric study. Series of parametric studies were conducted with the trained network model I in order to grasp a degree of effects of input parameters used in the neural network model on the output. For the objective of parametric study, five random value sets of other input parameters except one target parameter were selected in each possible range; for example, the sum of sand and silt and clay fractions is 100%, the compacted water content is from OMC−10(%) to OMC + 10(%), the void ratio is from 0.2 to 1.5, the friction angle is from 0° to 50°, and the cohesion is from 0 to 50 kPa. The parametric study was conducted by analyzing the trend of the ultimate increment of apparent cohesion ($C_{max}$) with the change in the object input parameter value for a possible range (Fig. 15). In other words, each line or symbol means the trend of $C_{max}$ with the variation of one target parameter at each random value set of other input parameters.

As shown in Fig. 15, the predicted ultimate increment of apparent cohesion ($C_{max}$) is higher when the sand fraction is lower, the silt and clay fractions are higher, and the cohesion is higher. The predicted ultimate increment of apparent cohesion ($C_{max}$) is higher when the void ratio and the friction angle are smaller, and the

Table 5
Connection weights and biases for the trained neural network models

| Model | | First layer | | Second layer | Input parameters |
|---|---|---|---|---|---|
| I | weight | −0.2283 | 0.5716 | | |
| | | 0.3734 | −0.8953 | | 1. sand fraction |
| | | −0.0006 | 0.5780 | 0.7042 | 2. silt & clay fraction |
| | | 0.2135 | −0.7207 | −1.6356 | 3. void ratio |
| | | 0.3002 | −1.3423 | | 4. water content |
| | | −0.1902 | 0.2060 | | 5. cohesion |
| | bias | 0.1067 | | 0.4168 | 6. friction angle |
| | | 0.0559 | | | |
| II | weight | 0.7160 | −0.1176 | | |
| | | −1.2468 | 0.3620 | | 1. sand fraction |
| | | 1.0797 | 0.4856 | −1.9650 | 2. silt & clay fraction |
| | | −0.7721 | 0.4552 | 1.0457 | 3. void ratio |
| | | −2.0471 | −0.4136 | | 4. water content |
| | bias | 0.1356 | | 0.5148 | 5. cohesion |
| | | −0.1327 | | | |
| III | weight | −0.2455 | 0.5476 | | |
| | | 0.4246 | −0.9349 | 0.7904 | 1. sand fraction |
| | | 0.2264 | −0.6780 | −1.6152 | 2. silt & clay fraction |
| | | 0.4942 | −1.2800 | | 3. water content |
| | | 0.0045 | 0.1442 | | 4. cohesion |
| | bias | 0.1138 | | 0.3484 | 5. friction angle |
| | | −0.2641 | | | |
| IV | weight | 0.4800 | 0.3216 | | |
| | | −0.8148 | −0.4444 | −1.5251 | 1. sand fraction |
| | | −0.4776 | 0.0342 | −0.5376 | 2. silt & clay fraction |
| | | 1.2251 | −0.3492 | | 3. void ratio |
| | | 0.0222 | 0.2051 | | 4. cohesion |
| | bias | −0.0669 | | 0.9382 | 5. friction angle |
| | | −0.0977 | | | |

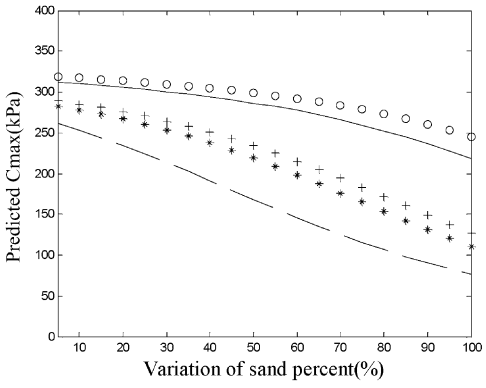


(a) Trend of $C_{max}$ with variation of sand fraction

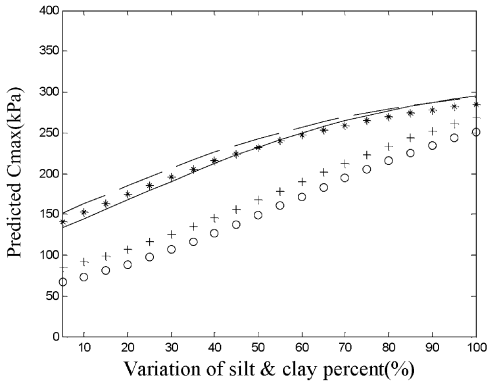


(b) Trend of $C_{max}$ with variation of silt and clay fraction

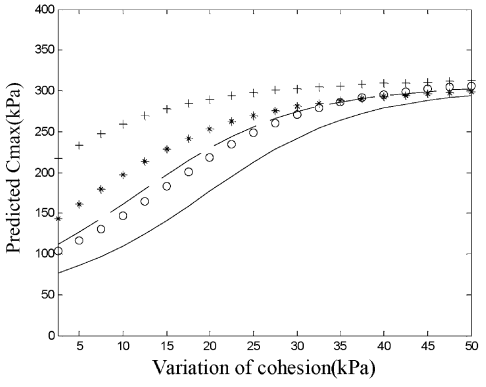


(c) Trend of $C_{max}$ with variation of cohesion( $c'$ )

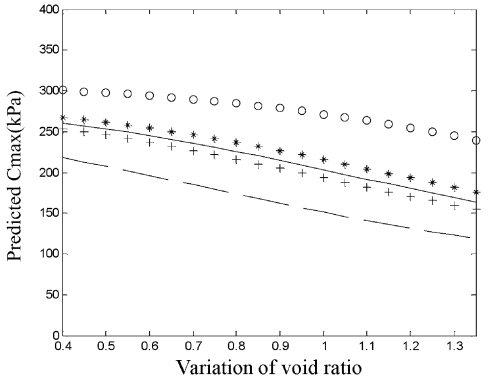


(d) Trend of $C_{max}$ with variation of void ratio

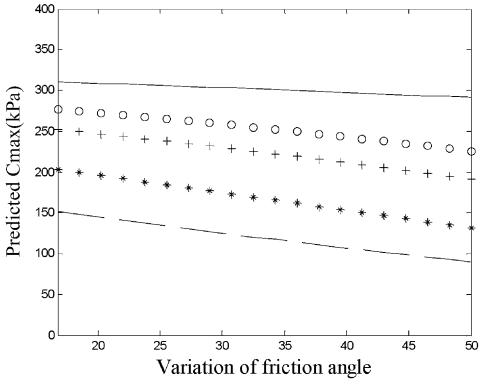


(e) Trend of $C_{max}$ with variation of friction angle( $\phi'$ )

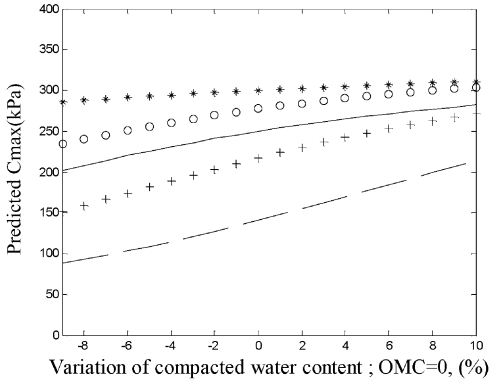


(f) Trend of $C_{max}$ with variation of compacted water content($w$)

Fig. 15. Parametric study results.

specimen is compacted at the wet side of OMC, even if the effect of them was relatively small.

## 4. Conclusions

In order to more reasonably understand the behavior of unsaturated soils, it is necessary to consider the increase in shear strength induced by the matric suction. In this paper, we proposed a simple but reliable method that could more effectively predict the unsaturated shear strength with respect to the matric suction.

First, we formulated a nonlinear hyperbolic equation containing only one more empirical parameter ($C_{max}$) for the purpose of representing the unsaturated shear strength. Validation of the proposed equation was

shown with regard to the published data and the test results obtained in this study. It has been found that the proposed hyperbolic formulation could well reproduce the apparent cohesion of unsaturated soils, increasing nonlinearly with the increase in the matric suction.

Based on the collected data as well as data obtained from this study, an interrelationship between the basic soil properties that can be measured easily and the ultimate increment of apparent cohesion ($C_{max}$) could be acquired using the ANN. We were also able to understand the degree of effects of the input parameters used in the neural network on the output by conducting a parametric study.

Furthermore, the network model resulted in relatively reliable predictions of $C_{max}$, even though new input parameter data were given in the trained network. The apparent cohesion obtained from ANN and hyperbolic equation was very reliable, even though the unsaturated shear strength data used in this work had been obtained from various kinds of soils and equipments.

Grouping soils by type and considering them respectively would lead to more effective applications of the ANN in the prediction of the unsaturated shear strength. In virtue of this work, it is expected that the problem of limited use of unsaturated shear strength can be solved and this nonlinear unsaturated shear strength modeling can be easily adopted in existing geotechnical analysis methods by simple modifications.

## Acknowledgements

The research reported in this paper was supported by Smart Infra-structure Technology Center under the sponsorship of KOSEF (Korea Science and Engineering Foundation).

## References

[1] Abramento M, Carvalho CS. Geotechnical parameters for the study of natural slopes instabilization at Sierra do Mar-Brazilian Southeast. Proceedings of the 12th International Conference on Soil Mechanics and Foundation Engineering, Rio de Janeiro 1989;3:1599–602.
[2] Bishop AW. The principle of effective stress. Publication 32. Oslo: Norwegian Geotechnical Institute; 1959.
[3] Bishop AW, Alpan I, Blight GE, Donald IB. Factors controlling the shear strength of partly saturated cohesive soils. In: ASCE Res. Conf. Shear Strength of Cohesive Soils. Univ. of Colorado, Boulder; 1960. p. 503–32.
[4] Chan WT, Chow YK, Liu LF. Neural network: an alternative to pile driving formulas. Computers and Geotechnics 1995;17:135–56.
[5] Cui YJ, Delage P. On the elasto-plastic behaviour of an unsaturated silt, A. S. C. E.. Geotechnical Special Publication 1993;39:115–26.
[6] De-Campos TMP, Carrillo CW. Direct shear testing on an unsaturated soil from Rio de Janeiro. Proc 1st Int Conf Unsaturated Soils, Paris 1995:31–8.
[7] Demuth HB, Beale M. Neural network toolbox for use with Matlab version 4. 2000.
[8] Donald IB. Effective stress parameters in unsaturated soils. In: Proc. 4thAustralia–New Zealand Conf. Soil Mech. Found. Eng. Adelaide, South Australia; 1963. p. 41–46.
[9] Escario V, Juca J. Strength and deformation of partly saturated soils. Proceedings of the 12th International Conference on soil Mechanics and Foundation Engineering, Rio de Janeiro 1989;3:43–6.
[10] Escario V, Saez J. The shear strength of partly saturated soils. Geotechnique 1986;36(3):453–6.
[11] Foresee FD, Hagan MT. Gauss–Newton approximation to Bayesian learning. Proceedings of the International Joint Conference on Neural Networks 1997:1930–5.
[12] Fredlund DG, Morgenstern NR, Widger RA. The shear strength of unsaturated soils. Canadian Geotechnical Journal 1978;15:313–21.
[13] Fredlund DG, Rahardjo H. Soil mechanics for unsaturated soils. New York: John Wiley & Sons Inc; 1995.
[14] Fredlund DG, Rahardjo H, Gan JKM. Nonlinearity of strength envelope for unsaturated soils. Proc 6th Int Conf Expansive Soils, New Delhi 1987;1:49–54.
[15] Gan JKM, Fredlund DG, Rahardjo H. Determination of the shear strength parameters of an unsaturated soil using the direct shear test. Canadian Geotechnical Journal 1988;25:500–10.
[16] Goh ATC. Pile driving records reanalyzed using neural networks. Journal of Geotchnical Engineering, ASCE 1996;122(6):492–5.
[17] Hagan MT, Demuth HB, Beale M. Neural network design. PWS Publishing Company; 1996.
[18] Hilf JW. An investigation of pore pressures in compacted cohesive soils. Technical memorandum 654, US Department of the Interior Bureau of Reclamation, Denver, Colorado, 1956.
[19] Ho DYF, Fredlund DG. Strain rates for unsaturated soil shear strength testing. Proc, 7th Southeast Asian Geotech Conf (Hong Kong), Nov 1982:787–803.
[20] Hornik K, Stinchcombe M, White H. Multilayer feed-forward networks are universal approximators. Neural Networks 1989;2(5):359–66.
[21] Karube D. New concept of effective stress in unsaturated soil and its proving test. Advanced Triaxial Testing of Soil and Rock. Philadelphia: ASTM STP 977, American Society for Testing and Materials; 1988.
[22] Khalili N, Khabbaz MH. A unique relationship for for the determination of the shear strength of unsaturated soils. Geotechnique 1998;48(5):681–7.
[23] Kim CY, Bae GJ, Hong SW, Park CH, Moon HK, Shin HS. Neural network based prediction of ground surface settlements due to tunneling. Computers and Geotechnics 2001;28:517–47.
[24] Krahn J, Fredlund DG, Klassen MJ. Effect of soil suction on slope stability at Notch Hill. Canadian Geotechnical Journal 1989;26(2):269–78.
[25] Lee IM, Lee JH. Prediction of pile bearing capacity using artificial neural networks. Computers and Geotechnics 1996;18(3):189–200.
[26] Lee IM, Sung SG, Yang IS. Characteristics and prediction of shear strength for unsaturated residual soil. In: Korean Geotechnical Society, 2000 Fall National Conference. 2000. p. 377–84.
[27] Lee SJ, Lee SR. Unsaturated shear strength characteristics of weathered granite soils. Korean Society of Civil Engineers 2002;22(1):81–8.
[28] Lee SR, Lee SJ, Byeon WY, Jang BS. Slope stability analysis by optimization technique considering unsaturated strength and SWCC. In: Proceedings of The Fourteenth KKNN Symposium on Civil Engineering. Kyoto, Japan; 2001. p. 563–8.

[29] MacKay DJC. Bayesian interpolation. Neural Computation 1992;4(3):415–47.
[30] MacKay DJC. A practical bayesian framework for back-propagation networks. Neural Computation 1992;4(3):448–72.
[31] Najjar YM, Basheer IA, Naouss WA. On the identification of compaction characteristics by neuronets. Computers and Geotechnics 1996;18(3):167–87.
[32] Öberg AL, Sällfors G. Determination of Shear strength parameters of unsaturated silts and sands based on the water retention curve. Geotechnical Testing Journal 1997;20(1):40–8.
[33] Pachepsky YA, Timlin D, Varallyay G. Artificial neural networks to estimate soil water retention from easily measurable data. Soil Science and Society of America J 1996;60:727–33.
[34] Penumadu D, Zhao R. Triaxial compression behavior of sand and gravel using artificial neural networks (ANN). Computers and Geotechnics 1999;24(3):207–30.
[35] Rafiq MY, Bugmann G, Easterbrook DJ. Neural network design for engineering applications. Computers and Structures 2001;79:1541–52.
[36] Rahardjo H, Lim TT, Chang MF, Fredlund DG. Shear-strength characteristics of a residual soil. Canadian Geotechnical Journal 1995;32:60–77.
[37] Rahman MS, Wang J, Deng W, Carter JP. A neural network model for the uplift capacity of suction caissons. Computers and Geotechnics 2001;28(4):269–87.
[38] Rassam DW, Williams DJ. A relationship describing the shear strength of unsaturated soils. Canadian Geotechnical Journal 1999;36(2):363–8.
[39] Ryu CH. Characteristics of permeability and strength for Unsaturated granite weathered soils. PhD thesis, Dongguk University, South Korea, 1997.
[40] Satija BS. Shear behaviour of partly saturated soils. PhD thesis, Indian Institute of Technology, Delhi; 1978.
[41] Satija BS, Gulhati. Strain rate for shearing testing of unsaturated soil. In: Proc. 6th Asian Reg. Conf. Soil. Mech. Found. Eng. Singapore; 1979. p. 83–6.
[42] Shin HS, Pande GN. On self-learning finite element codes based on monitored response of structures. Computers and Geotechnics 2000;27(3):161–78.
[43] Sidarta DE, Ghaboussi J. Constitutive modeling of geomaterials from non-uniform material tests. Computers and Geotechnics 1998;22(1):53–71.
[44] Vanapalli SK, Fredlund DG, Pufahl DE, Clifton AW. Model for the prediction of shear strength with respect to soil suction. Canadian Geotechnical Journal 1996;33(3):379–92.